JOURNAL OF MATERIALS SCIENCE 29 (1994) 4933–4940

# Effect of microstructure on the fatigue strength of an austempered ductile iron

P. SHANMUGAM, P. PRASAD RAO, K. RAJENDRA UDUPA, N. VENKATARAMAN
*Department of Metallurgical Engineering, Karnataka Regional Engineering College, Surathkal, Karnataka 574157, India*

Rotating bending fatigue tests were carried out on austempered ductile iron containing 1.5 wt% nickel and 0.3 wt% molybdenum. The ductile iron was austenitized at 900 or 1050 °C and then austempered at 280 or 400 °C for different lengths of time to obtain different microstructures. The fatigue strength was correlated with the amount of retained austenite and its carbon content, which were both determined by X-ray diffraction technique. While the tensile strength decreased with increasing retained austenite content, the fatigue strength was found to increase. Carbide precipitation was found to be detrimental to fatigue strength. Lower austenitizing temperature resulted in better fatigue strength.

## 1. Introduction

In recent years, austempered ductile irons (ADI) have been used for many critical components in automobiles [1–3], such as crank shafts, steering knuckles and hypoid rear axle gears. It is expected that the application of these irons will increase in the future, not only in the automobile industry, but also in many other fields. The interest in these irons is due to the fact that they offer an exceptional combination of high strength, ductility and toughness. This unusual combination of properties comes about because of their unique microstructure, which consists of ferrite and austenite, rather than ferrite and carbide, as in austempered steels [4].

The presence of appreciable amounts of austenite should lead to better wear resistance and fatigue strength in these, due to the high work-hardening nature of the austenite. While considerable work has been done in understanding the microstructural characteristics of a number of ADIs and their effect on tensile properties [5], impact toughness [6] and fracture toughness [7], rather limited information is available on their effect on fatigue properties. One of the earliest investigations is that of Johansson [8]. He carried out rotating bending fatigue tests on notched and unnotched specimens which showed that fatigue strengths of ADI were far superior to those of pearlitic and "quenched and tempered" grades. However, the report lacks information on heat treatment and microstructural details, which would be helpful in understanding the correlation between microstructure and fatigue strength. Limited reports are available on other investigations of fatigue characteristics, and these have been summarized by Harding [5].

The present investigation was undertaken to evaluate systematically the microstructure and fatigue strength of austempered ductile iron with a view to establishing the correlation between these two.

## 2. Experimental procedure

The alloy for the present study was produced at M/s Shanthala Ductile Iron Foundry, Shimoga. The foundry practice followed is given elsewhere [9]. The complete chemical analysis is presented in Table 1.

Samples for X-ray diffraction, tensile and fatigue tests were machined from the cast slabs. The dimensions of the fatigue and tensile samples are given in Fig. 1. X-ray diffraction studies were carried out on samples of dimensions 30 mm × 25 mm × 3 mm.

Austempering heat treatment consisted of three variables: austenitizing temperature, austempering temperature and austempering time. Through appropriate selection of these variables, different microstructures and mechanical properties were obtained. Heat-treatment combinations employed in the present investigation are illustrated in Fig. 2. The fourth parameter, of austenitizing time, was kept constant at 60 min for all heat treatments. All the samples were plated with copper prior to heat treatment to minimize surface oxidation. Austenitization was carried out in a flowing argon atmosphere while austempering treatment was carried out in salt bath of a mixture of 45% sodium nitrate and 55% potassium nitrate by weight. Temperature was controlled to better than ± 2 degrees of the set point.

Tensile and fatigue samples were subjected to buffing after heat treatment, to give them a high degree of surface finish. Four grades of abrasive powders were used: 80, 120, 240 and finished with 500 grit. Fatigue samples were subjected to longitudinal polishing. The samples for X-ray diffraction were initially subjected to a mechanical polish and then to electropolishing to remove a surface layer of at least 50 μm.

X-ray diffraction studies were carried out on a Jeol-JDX-8P diffractometer using a copper target and nickel filter, at a scan speed of 0.25° $min^{-1}$ over an angular range of 40°–45° 2θ. Hardness studies were

0022–2461 

TABLE I Chemical analysis of the iron

| Element | (wt%) |
|---|---|
| C | 3.75 |
| Si | 2.29 |
| Mn | 0.374 |
| S | 0.014 |
| P | 0.34 |
| Mg | 0.04 |
| Ni | 1.41 |
| Mo | 0.32 |

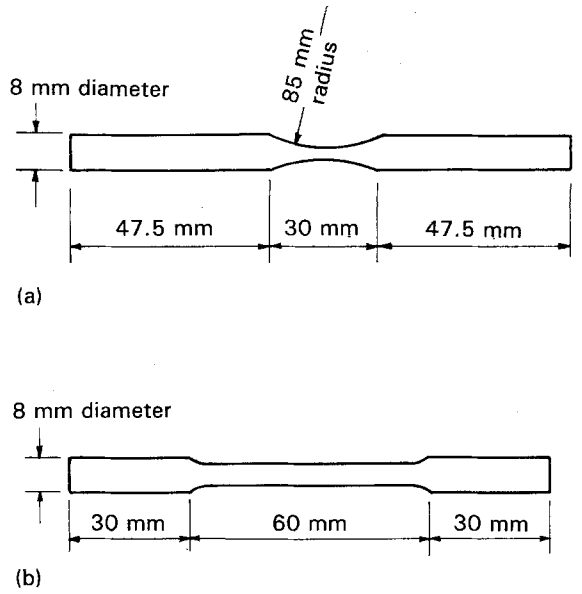


*Figure 1* Dimensions of (a) fatigue and (b) tensile samples.

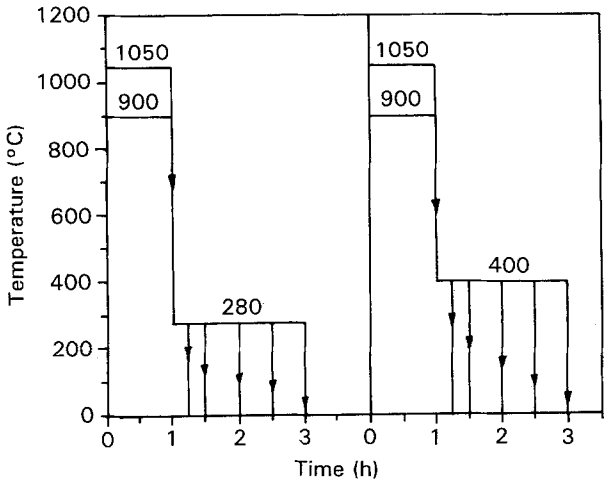


*Figure 2* Heat-treatment schedules employed.

carried out on a Zwick Vickers hardness tester using a load of 10 kg. Tensile tests were carried out on an Instron 4206 floor model machine at a strain rate of $1.4 \times 10^{-4}$ s$^{-1}$. The results reported are an average of at least three samples.

Fatigue tests were carried out in rotating bending fatigue testing machines using double-point load, at a frequency of 1400 cycles/min. $S$–$N$ curves were established for different heat-treatment conditions. Fatigue limit was taken as that stress value at which the sample endured at least $10^6$ cycles. Five tests were carried out at each stress level, and the results reported are an average of these five tests.

## 3. Results

Optical microscopy revealed that the samples austempered at 280 °C had acicular morphology, while those austempered at 400 °C had a feathery morphology. It was further noticed that austenitizing at 1050 °C resulted in longer bainitic needles or feathers than at 900 °C. A set of typical microstructures is shown in Figs 3 and 4.

X-ray diffraction studies were carried out to estimate (i) the initial carbon content of austenite, (ii) the volume fraction of different phase constituents in austempered samples, and (iii) the carbon content of retained austenite. The initial carbon content of the austenite was determined by the method proposed by Rundman and Klug [10]. Analysis of (2 1 1) diffraction peaks of martensite yielded carbon percentages of 0.75% and 1.035% in the samples quenched from 900 and 1050 °C, respectively.

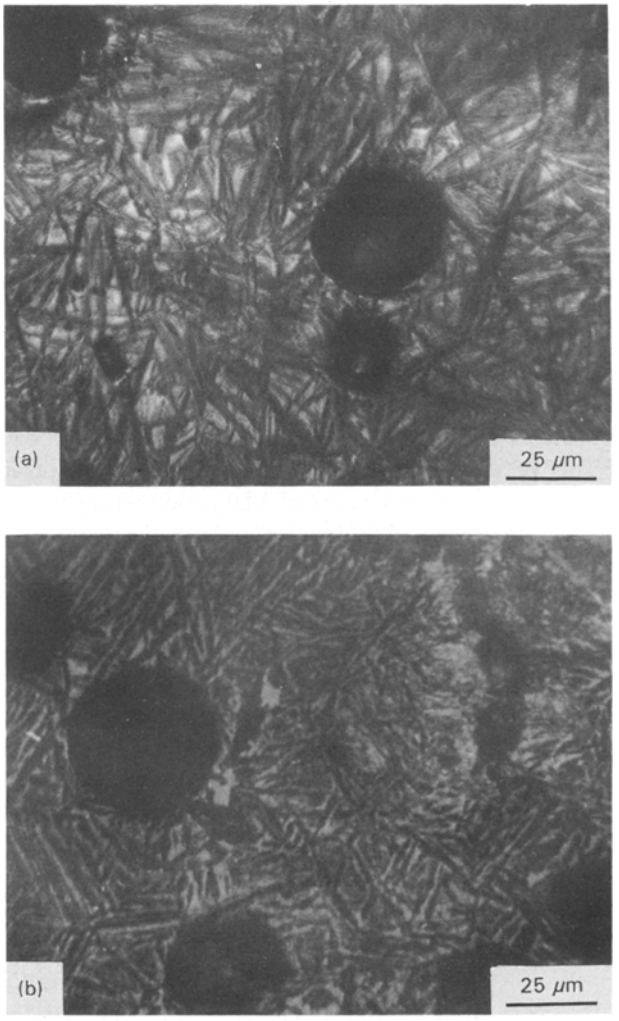


*Figure 3* Microstructures of samples austenitized at 1050 °C and then austempered for 60 min at (a) 280 °C, and (b) 400 °C.

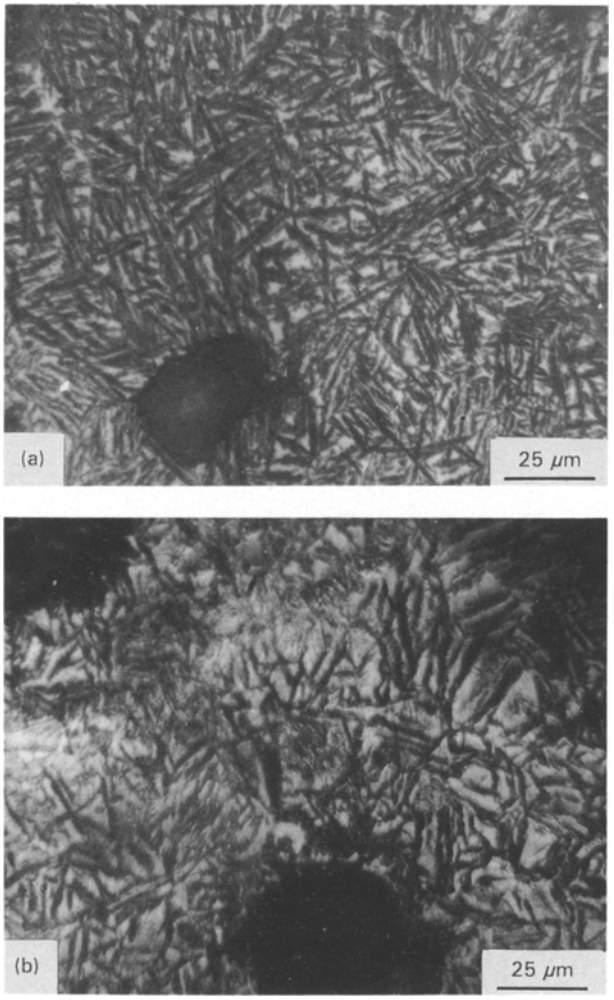


*Figure 4* Microstructures of samples austenitised at 900 °C and then austempered for 60 min (a) 280 °C, and (b) 400 °C.

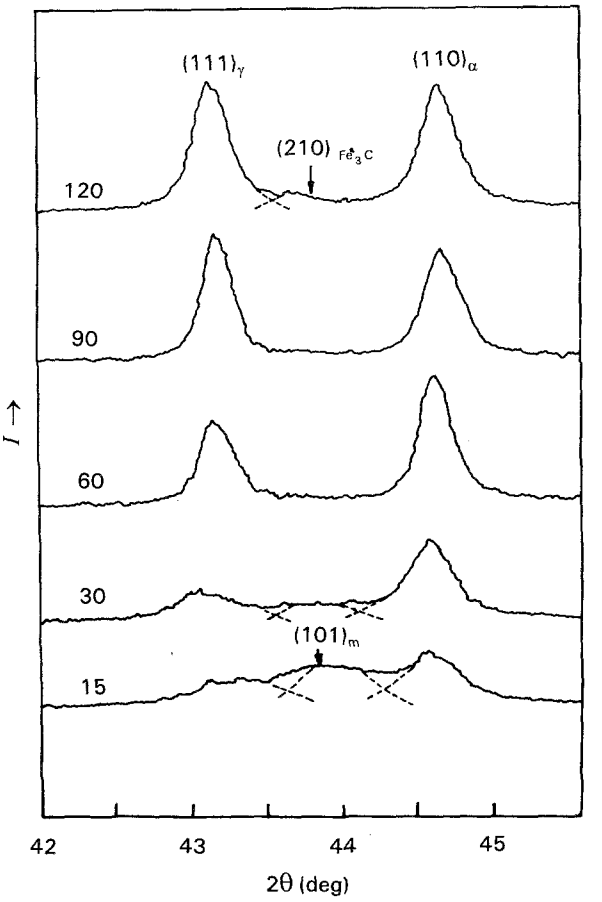


*Figure 5* Diffraction profiles of samples austenitized at 900 °C and austempered at 400 °C. Austempering periods (min) are shown on the profiles.

Cullity's [11] direct comparison method was employed for estimating the volume fractions of phase constituents. Fig. 5 shows a typical set of diffraction profiles. At short austempering time, peaks due to austenite, martensite and ferrite were observed. A simple unfolding technique was employed [12] to separate these. While the martensite peak shrank with increasing austempering time, the austenite and ferrite peaks expanded. In samples austempered at 400 °C for 120 min, an additional peak was seen to emerge close to the austenite peak, due to the carbide precipitation. The proportions of phases in the samples austempered under different conditions are given in Table II. The variation of volume fraction of retained austenite with austempering time is shown in Fig. 6.

It was found that there was a considerable shift in the position of the austenite peak with austempering time, showing a systematic increase in lattice parameter. The carbon content of retained austenite was estimated from the relation between its lattice parameter and carbon content. The variation of carbon content with austempering time so obtained is shown in Fig. 7. It is found that the carbon content initially increases with increasing time, and then decreases beyond 90 min austempering.

Variation of hardness with austempering time under different heat-treatment schedules are shown in Fig. 8. Generally, hardness was found to decrease with increasing austempering time and temperature. A gradual rise in hardness is discernible beyond austempering periods of 90 min.

The variation of tensile strength with austempering time is shown in Fig. 9. The trend is similar to that found for hardness.

*S–N* curves were determined for samples austempered for different austempering times at the austenitizing/austempering temperature combinations of 900/400, 1050/280 and 1050/400. No fatigue studies were conducted on samples subjected to a heat-treatment combination of 900/280, as these showed little variation in retained austenite content with austempering time. The results of the fatigue tests are shown in Figs 10–12. A smooth curve was drawn through the data points rather than a straight line, as it fitted the data points better. Arrows on data points indicate that the samples did not fail even after $10^6$ cycles. The highest stress at which the samples endured $10^6$ cycles was taken as the fatigue strength. The variation of fatigue strength with austempering time is shown in Fig. 13. For heat-treatment combinations of 900/400 and 1050/280, it is found that fatigue strength increases with increasing austempering time. However, the samples subjected to a heat-treatment combination of 1050/400 show a different behaviour. The fatigue strength increases initially, reaches a plateau and then falls.

TABLE II Volume fraction of phase constituents in the austempered samples

| Austenitizing Temp. (°C) | Austempering | | Retained austenite (%) | Bainitic ferrite (%) | Martensite (%) | Carbide precipitation |
|---|---|---|---|---|---|---|
| | Temp. (°C) | Time (min) | | | | |
| 900 | 280 | 15 | – | – | – | |
| | | 30 | – | – | – | |
| | | 60 | 7 | 93 | – | |
| | | 90 | 9 | 91 | – | |
| | | 120 | 9.5 | 90.5 | – | |
| | 400 | 15 | 17 | 68 | 15 | |
| | | 30 | 20 | 80 | Trace | |
| | | 60 | 27 | 73 | | |
| | | 90 | 37 | 63 | | |
| | | 120 | 36 | 64 | | Trace |
| 1050 | 280 | 15 | 15 | 65 | 20 | |
| | | 30 | 30 | 52 | 18 | |
| | | 60 | 40 | 60 | Trace | |
| | | 90 | 45 | 55 | | |
| | | 120 | 51 | 49 | | |
| | 400 | 15 | 9 | 56 | 35 | |
| | | 30 | 16 | 84 | Trace | |
| | | 60 | 19 | 81 | | |
| | | 90 | 22 | 78 | | |
| | | 120 | 29 | 71 | | Trace |

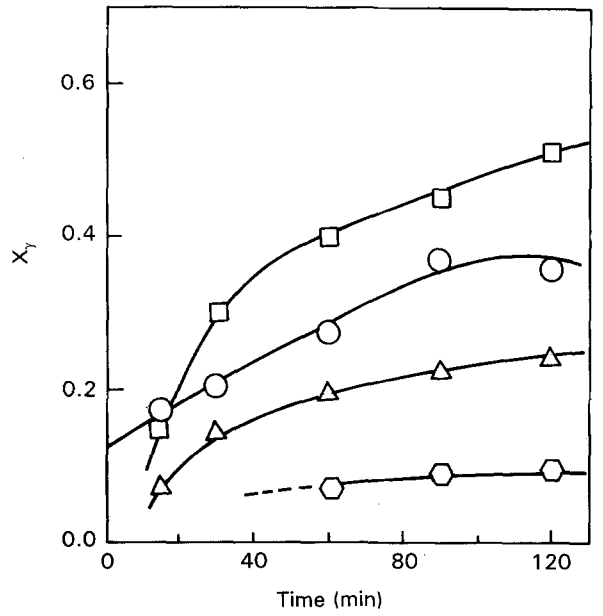


*Figure 6* Variation of volume fraction of retained austenite with austempering time. (○) 900/280, (○) 900/400, (□) 1050/280, (△) 1050/400.

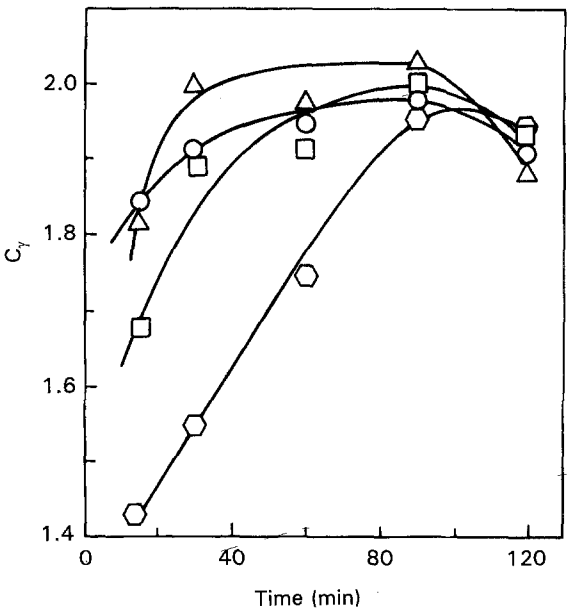


*Figure 7* Variation of carbon content of retained austenite with austempering time. For key, see Fig. 6.

## 4. Discussion

The microstructures of austempered samples confirm the TTT diagram established by Janowak and Morton [13] for ductile iron containing 1.5Ni and 0.3Mo when austenitized at 900 °C. Because the work of Janowak and Morton further establishes that changing the austenitizing temperature alters only the time duration of the bainitic reaction and not the temperature range, similar bainitic morphology is expected at the two austenitizing temperatures. However, the higher austenitizing temperature resulted in longer bainitic needles due to the coarser prior austenite grains.

The variation of volume fraction of phase constituents was found to depend on the heat-treatment temperatures. These could be explained in a qualitative way, based on our present understanding of the bainitic reaction in ADI [4]. Consider first the samples austenitized at 900 °C. The high growth rate of bainitic ferrite needles and low diffusion rate of carbon results in a low retained austenite content at the low temperature of 280 °C. It is only about 7%–10% and increases only gradually with time. But at 400 °C, the higher diffusion rate of the carbon leads to carbon enrichment of the austenite region between the bainitic ferrite needles. As can be seen from Fig. 7, carbon

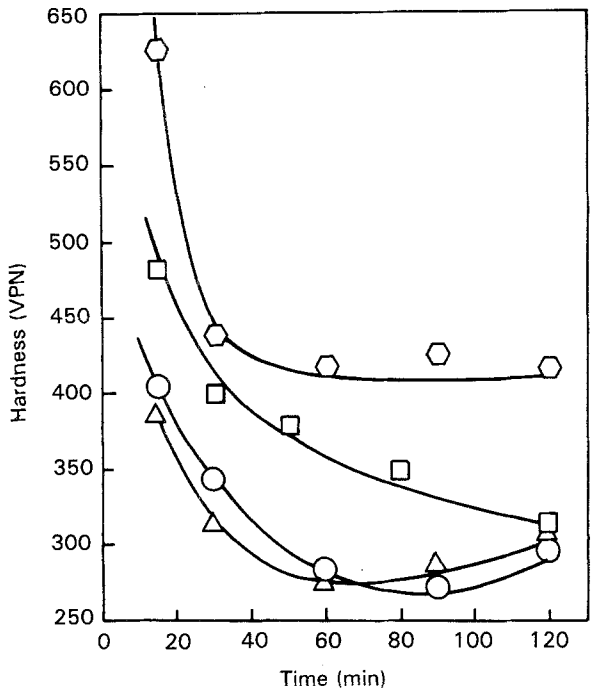


*Figure 8* Variation of hardness with austempering time. For key, see Fig. 6.

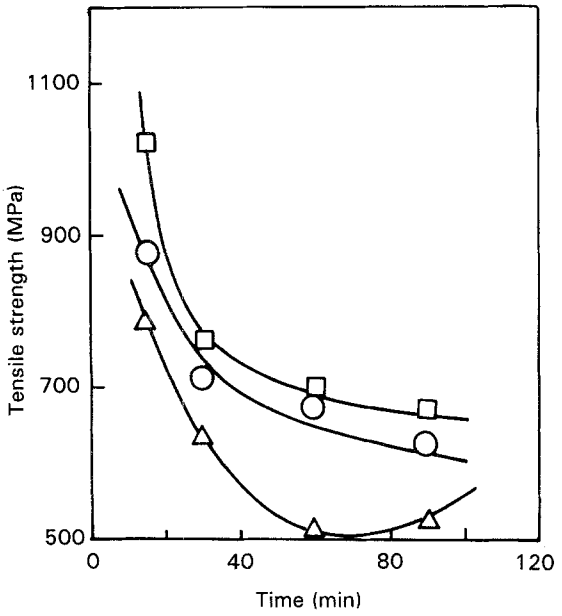


*Figure 9* Variation of tensile strength with austempering time. (○) 900/400, (□) 1050/280, (△) 1050/400.

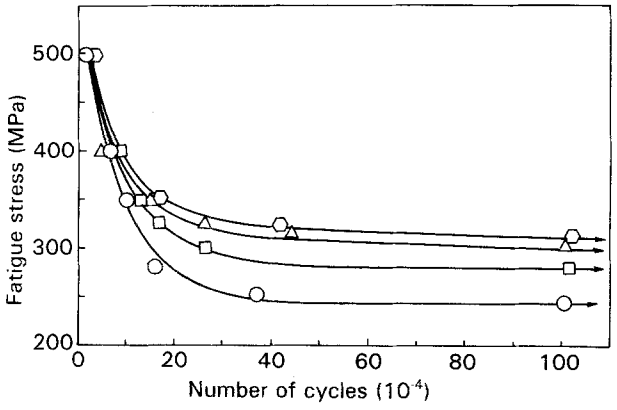


*Figure 10* S–N curves for samples austenitized at 1050 °C and austempered at 280 °C for various durations: (○) 15, (□) 30, (△) 60, (◇) 90 min.

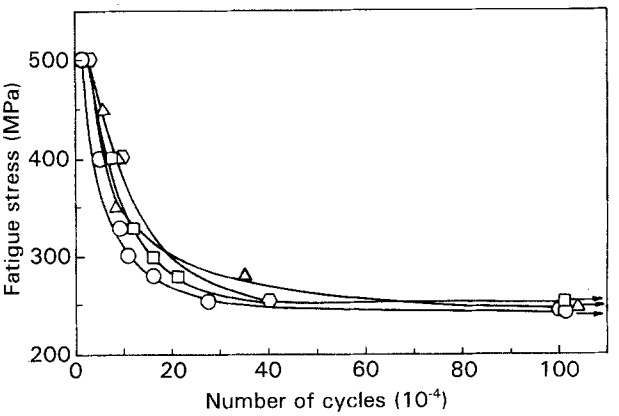


*Figure 11* S–N curves for samples austenitized at 1050 °C and austempered at 400 °C for various durations. For key, see Fig. 10.

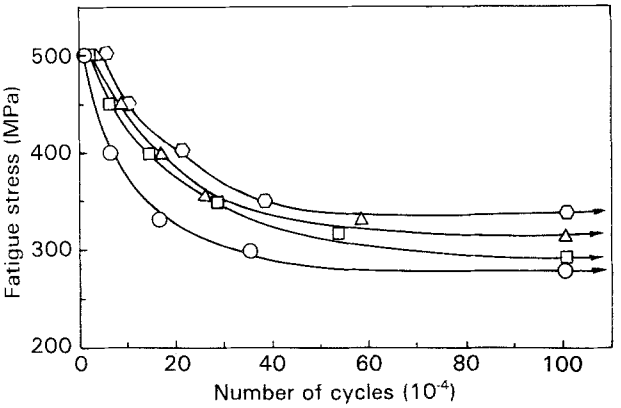


*Figure 12* S–N curves for samples austenitized at 900 °C and austempered at 400 °C for various durations. For key, see Fig. 10.

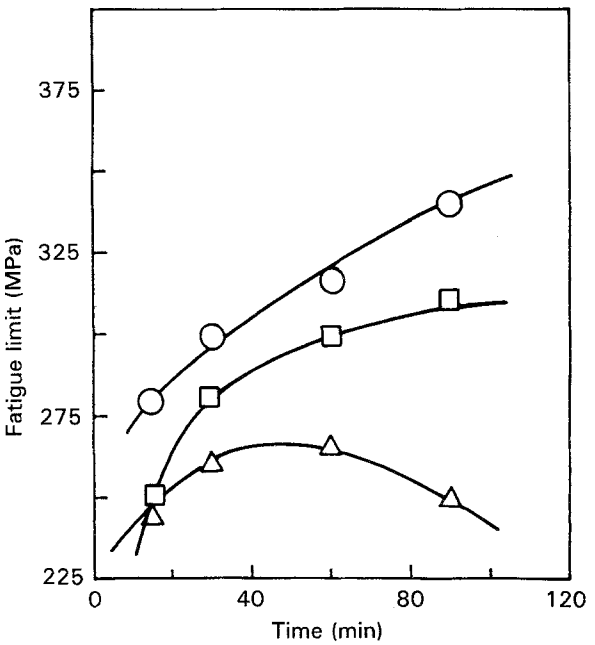


*Figure 13* Variation of fatigue strength with austempering time. For key, see Fig. 9.

content of the austenite rises very quickly to values nearly equal to 2.0%. As a result, the amount of retained austenite increases sharply. The fact that almost all the carbon in the matrix is now transferred to the retained austenite is indicated by Fig. 14. Here

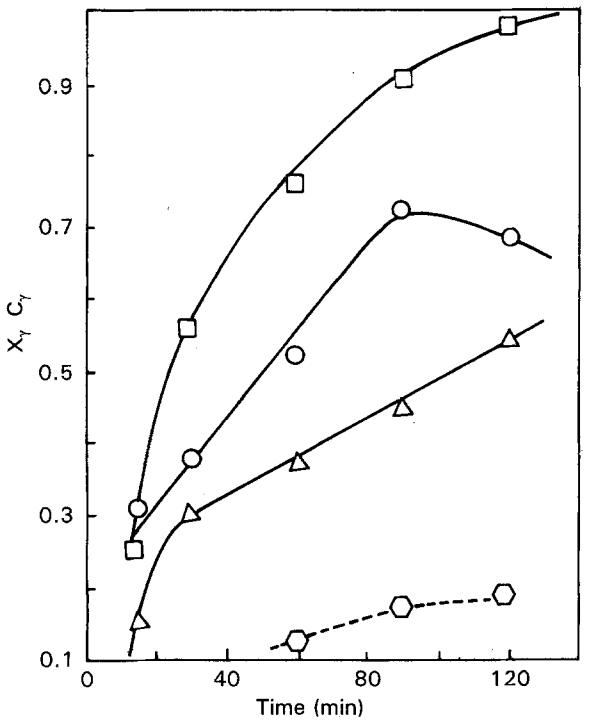


*Figure 14* Variation of $X_\gamma C_\gamma$ with austempering time. For key, see Fig. 6.

the product $X_\gamma C_\gamma$, the total carbon content of retained austenite, reaches almost 0.75%, the same as the original matrix carbon content. In contrast, at 280 °C, very little carbon is transferred to austenite.

When samples are austenitized at 1050 °C, we see a different picture. The amount of retained austenite is observed to be higher when austempered at 280 °C rather than at 400 °C (see Fig. 6). Because of the higher matrix carbon content, sufficient carbon build up takes place ahead of the growing bainitic ferrite needle even at 280 °C, very quickly building up to values exceeding 2%. This leads to appreciable retention of austenite. The amounts of retained austenite estimated are even higher than those for 900/400 and exceed 50 vol % after 90 min. The matrix carbon approaches the total carbon content of 1.04%.

However, at 1050/400, the higher carbon content of the austenite, together with faster diffusion of carbon from growing bainitic ferrite needles, leads to rapid increase in carbon content of the austenite as can be seen from Fig. 7. The carbon content of retained austenite reaches a value of 2.0 wt % within 30 min. Beyond that, there is a gradual but steady decrease in the carbon content. The decrease becomes rapid beyond 90 min. This indicates carbide precipitation during the so-called second stage of bainitic reaction [4]. Even though the decreasing carbon content of the austenite indicates carbide precipitation, it could only be detected by X-ray diffraction technique after 120 min. At shorter durations, the amount of carbide is too low to give any appreciable intensity to the diffraction peaks. The detection of carbide peaks is difficult because their strongest peak (1 0 3) overlaps the ferrite (1 1 0) peak and the second strongest peak (2 1 0) lies very close to the austenite (1 1 1) peak.

TABLE III Fatigue ratios under different heat-treatment conditions

| Austenitizing temp. (°C) | Austempering temp. (°C) | Fatigue ratio | | | |
|---|---|---|---|---|---|
| | | Austempering time (min) | | | |
| | | 15 | 30 | 60 | 90 |
| 900 | 400 | 0.29 | 0.42 | 0.47 | 0.54 |
| 1050 | 280 | 0.22 | 0.36 | 0.43 | 0.46 |
| | 400 | 0.34 | 0.41 | 0.51 | 0.48 |

Both hardness and tensile strength decrease with increasing austempering time and temperature, as shown in Figs 8 and 9, respectively. Strength and hardness decrease as the retained austenite content increases. The high initial hardness and strength is due to some amount of martensite which is present in the microstructure. The gradual rise in hardness and strength during late stages of austempering is due to carbide precipitation.

While hardness and tensile strength decrease with increasing austempering time, fatigue strength increases as shown in Fig. 13. 900/400 treatment gives higher fatigue strength than 1050/280 heat treatment. The samples subjected to 1050/400 treatment showed low fatigue strength which started decreasing after 60 min. Fatigue strengths of samples subjected to 900/280 treatment were not investigated.

It is generally reported for steels and other materials that fatigue strength decreases with decreasing tensile strength [14]. However, in the austempered ductile irons, it is found that fatigue strength increases as the tensile strength decreases. The fatigue ratio, which is defined as the ratio of fatigue limit to tensile strength, increases from low values of about 0.2 to high values of about 0.5 as the austempering time is increased. The fatigue ratios obtained under different heat treatments are listed in Table III.

The unusual phenomenon of increasing fatigue strength with decreasing tensile strength, is undoubtedly related to such microstructural parameters as $X_\gamma$, and $C_\gamma$. Therefore, fatigue limit was plotted against the product $X_\gamma C_\gamma$ as shown in Fig. 15. Two linear curves are obtained. The results of the heat treatments 1050/280 and 1050/400 fall on one curve, while that of 900/400 falls on another, with a steeper slope. For the same matrix carbon content, austenitizing at 900 °C gives higher fatigue strength than at 1050 °C.

Lowering the austenitizing temperature has a number of implications for the microstructure. First of all, it leads to lower prior austenitic grain size which in turn leads to smaller bainitic needles. Secondly, a lower austenitizing temperature leads to a lower initial carbon content in the austenite. Therefore, during austempering, the carbon content rises more slowly, as seen from Fig. 7. For a given austempering temperature and time, samples austenitized at lower temperature have lower carbon content. Thirdly, a lower austenitizing temperature gives a homogeneous carbon distribution in the prior austenite and will

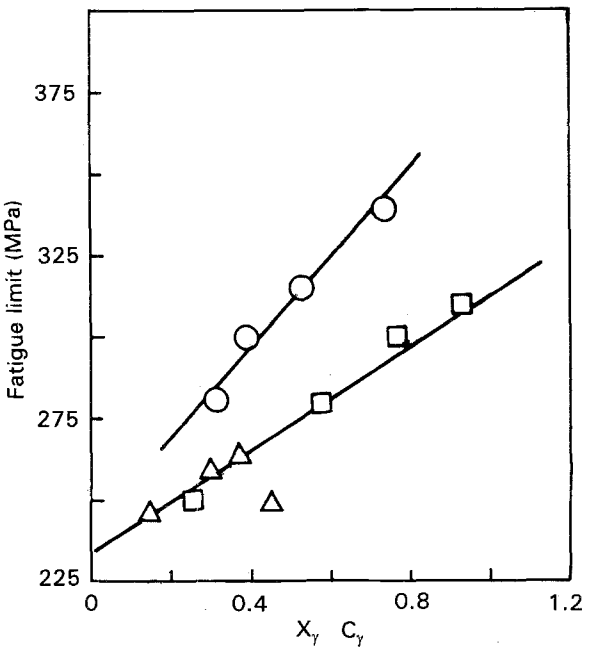


*Figure 15* Variation of fatigue strength with $X_\gamma C_\gamma$. For key, see Fig. 9.

suppress its segregation at cell boundaries [15, 16]. This will lead to improved toughness.

The fatigue strength increases with the retained austenite content because of its higher strain-hardening behaviour. The excellent strain-hardening behaviour of austenite is well known, a typical example being Hadfield manganese steel. There may be strain-induced martensite formation in some austenitic steels. This is not likely to occur in the austempered ductile iron because of its high carbon content. This lowers the $M_s$ temperature substantially. It is reported [2] that the $M_s$ temperature may be as low as $-120\,^{\circ}C$. Owing to the high strain-hardening nature of the retained austenite, the formation of persistent slip bands will be delayed. This will delay the nucleation of fatigue crack. Therefore, both at 1050/280 and 900/400, we see that the fatigue strength increases with increasing austempering time, because retained austenite content increases with austempering time. However, at 1050/400, after an initial rise, the fatigue strength reaches a plateau, and then decreases. From X-ray diffraction data it was observed that carbide precipitation occurred after about 90 min austempering. It is clear that the precipitation of these carbides is detrimental to the fatigue properties.

The increase in fatigue strength is enhanced further by the interstitial carbon which is present in retained austenite in large amounts. The interstitial carbon induces strain ageing. This increases with increasing carbon content, that is, with increasing austempering time. Thus we observe that fatigue strength increases with increasing $C_\gamma$ or $X_\gamma C_\gamma$.

We have seen that austenitizing temperature is an important factor. It is advisable to keep it low in order to obtain a finer bainite morphology. A lower austenitizing temperature will also prevent the retention of prior austenite due to carbon segregation at cell boundaries. A network of this retained prior austenite is undesirable, unlike the bainitic austenite. This is because the former can transform to martensite under strain. The presence of this strain-induced martensite will lead to a loss of toughness and reduction in fatigue strength.

It has been reported [15] that, in order to obtain good ductility, the austempering temperature must be such that an optimum amount of retained austenite is formed, say about 40%. As the austenitizing temperature is raised, this will necessitate a reduction in austempering temperature. Thus, while good fatigue strength was observed on austempering at 400 °C after austenitizing at 900 °C, austempering had to be at 280 °C for samples austenitized at 1050 °C. At the higher austenitizing temperatures, the high austempering temperatures are also undesirable due to the fact that they will lead to precipitation of carbides. As seen from the fatigue data for the samples heat treated at 1050/400, the carbide precipitation lowers the fatigue strength considerably.

Summarizing, it may be said that best fatigue results are obtained by (i) austenitizing at a lower temperature such that prior austenite grain size is small and segregation of carbon at cell boundaries is absent, and (ii) austempering at a moderate temperature such that there is a sufficiently large volume fraction of feathery bainite with a high matrix carbon content and free from carbide precipitation.

## 5. Conclusions

1. The fatigue strength increases with austempering time while the tensile strength decreases. This results in increasing fatigue ratio with increasing austempering time.
2. A lower austenitizing temperature results in improved fatigue strength. This can be interpreted in terms of prior austenitic grain size and carbon segregation at cell boundaries.
3. High retained austenite content and high matrix carbon content leads to high fatigue strength.
4. Carbide precipitation results in loss of fatigue strength.
5. Feathery bainite results in higher fatigue strength than acicular bainite.

## Acknowledgement

This work was financially supported by the Ministry of Human Resource Development, Government of India.

## References

1. J. DODD, *Mod. Casting* **68**(5) (1978)60.
2. R. B. GUNDLACH and J. F. JANOWAK, *Met. Progr.* **123** (1985) 119.
3. R. A. HARDING and G. N. J. GILBERT, *Brit. Foundryman* **79** (1986) 489.
4. J. JANOWAK and R. GUNDLACH, *AFS Trans.* **91** (1983) 377.
5. R. A. HARDING, *Met. Mater.* **2** (1986) 65.
6. R. C. VOIGT, *AFS Trans.* **91** (1983) 2253.
7. JI-LIANG DOONG and SHY-ING YU, *Int. J. Fatigue* **10** (1988) 219.

8. M. JOHANSSON, *AFS Trans.* **85** (1977) 117.
9. K. MUTHUKUMARAN, MTech thesis, Mangalore University (1990).
10. K. B. RUNDMAN and R. C. KLUG, *AFS Trans.* **90** (1982) 495.
11. B. D. CULLITY, "Elements of X-ray diffraction" (Addison-Wesley, Reading, MA, 1974) p. 411.
12. P. SHANMUGAM, MTech thesis, Mangalore University (1991).
13. J. F. JANOWAK and P. A. MORTON, Amax Report XGI-84-03, Amax Materials Research Centre, Ann Arbor, MI (1984).
14. G. E. DIETER, "Mechanical Metallurgy" (McGraw-Hill, London, 1988) p. 415.
15. R. B. GUNDLACH and J. F. JANOWAK, Amax Report XGI-84-02, Amax Materials Research Centre, Ann Arbor, MI (1984).
16. J. F. JANOWAK, R. B. GUNDLACH, G. T. ELDIS and K. ROHRIG, Official exchange paper, 48th International Foundry Congress, Varna, Bulgaria (1981).

*Received 26 March 1992*
*and accepted 31 August 1993*